Exocytosis of IgG as mediated by the receptor, FcRn: An analysis at the single-molecule level

Raimund J. Ober*†, Cruz Martinez*, Xuming Lai*†, Jinchun Zhou*, and E. Sally Ward*‡

*Center for Immunology, University of Texas Southwestern Medical Center, 6000 Harry Hines Boulevard, Dallas, TX 75390-8576; and †Department of Electrical Engineering, University of Texas at Dallas, Richardson, TX 75080

Edited by Pamela J. Bjorkman, California Institute of Technology, Pasadena, CA, and approved June 2, 2004 (received for review April 28, 2004)

IgG transport within and across cells is essential for effective humoral immunity. Through a combination of biochemical and *in vivo* analyses, the MHC class I-related neonatal Fc receptor (FcRn) is known to play a central role in delivering IgGs within and across cells. However, little is known about the molecular and cellular mechanisms that are involved in the exocytosis of IgG from cells that express FcRn. Here, we use single-molecule fluorescence microscopy to analyze exocytic processes in FcRn-GFP-transfected human endothelial cells. We show that exocytosis can occur by means of multiple modes that range from complete fusion of the exocytic vesicle with the plasma membrane to a slower-release mode ("prolonged release") that only involves partial mixing of membrane contents. Even for prolonged release, diffusion of FcRn into the plasma membrane can occur, indicating that FcRn is directly involved in IgG exocytosis. The slower-release mode is characterized by periodic, stepwise release of IgG, rather than the rapid burst that is observed for complete-fusion events. Analyses of single-molecule tracks suggest that IgG may be bound to FcRn for several seconds after exocytosis. Unexpectedly, after diffusion out of the exocytic site, IgG and FcRn molecules can also migrate back into the epicenter of the release site. Such retrograde movement may represent a mechanism for FcRn retrieval. Our studies provide insight into the events that lead to IgG exocytosis.

The transport of IgG across cellular barriers plays a central role in mediating effective humoral immunity. For example, IgG can cross epithelial and endothelial barriers of diverse origin by means of transcytosis (1–6). Here, we investigate the cellular processes that are involved in the exocytic delivery of intracellularly transported IgG into the extracellular space. This step represents a pivotal, yet poorly understood, part of the transport process.

Through biochemical and *in vivo* studies it is known that the MHC class I-related neonatal Fc receptor (FcRn) plays an important role in IgG transport (7). This Fc receptor, which is both structurally and functionally distinct from the Fcγ receptors (7, 8), has been shown to specifically transport IgG across cellular barriers (1–6, 9–12). Through its IgG transport function, FcRn appears to have multiple roles that include, but are not limited to, the delivery of maternal IgG to offspring (11, 13–16) and the regulation of serum IgG levels throughout life (17–19). However, little is known about the details of the mechanisms by which FcRn mediates trafficking of IgG within and across cells. By using fluorescence imaging techniques, it has been shown that FcRn sorts IgGs in the sorting endosome (20). Receptor-bound IgG molecules are either recycled or transcytosed. In contrast, molecules that do not bind to FcRn enter the lysosomal pathway and are ultimately degraded (21). Whether FcRn is directly involved in the exocytosis of IgG at the cell membrane is one of multiple unresolved questions concerning the role that FcRn plays in IgG trafficking.

Our focus in this study is to analyze the modes by which IgG is released from endothelial cells after uptake and recycling or transcytosis by FcRn. More generally, this analysis relates to a fundamental question in cell biology: what is the topology of exocytic vesicles and the plasma membrane during the release of exocytic cargo from cells? The classical model of exocytosis posits that the vesicular and plasma membranes fuse completely, and that this fusion is followed by endocytic retrieval of membrane and receptors at different sites (22). However, more recent studies (23–30) in systems of regulated exocytosis (e.g., neuronal, chromaffin, and endocrine cells) indicate that as an alternative to complete fusion, exocytosis can involve events that can be broadly categorized as "kiss and run." For kiss-and-run-type events, exocytosed material is released from the exocytic vesicle or tubule through a poorly characterized fusion pore that subsequently reseals. The net result is that (*i*) the exocytic compartment does not collapse into the membrane, and (*ii*) some membrane components are selectively retained (27–29). This mode of exocytosis has clear advantages for optimizing retrieval efficiency and may be particularly relevant when rapid release and retrieval cycles are needed (e.g., synaptic junctions; ref. 30).

To date, exocytic events have been primarily studied in systems of regulated release in specialized cell types (e.g., refs. 25–29 and 31–33). There is a paucity of data describing the modes of constitutive exocytosis that result in the release of recycled (or transcytosed) ligands in any system. It is conceivable that under less demanding conditions with respect to exocytic load and speed than those involved in regulated exocytosis, the more classical mode of exocytosis involving complete fusion of vesicular and plasma membranes might occur. Conversely, and with particular relevance to FcRn, incomplete fusion at the exocytic site might operate as an efficient way of maintaining low surface-expression levels of this receptor (1–5, 17). In the context of maintaining IgG homeostasis, the mode of exocytosis would also be expected to directly impact whether net uptake from the extracellular milieu or release of IgG occurs during the association of exocytic compartments with the plasma membrane.

We have used total internal reflection fluorescence microscopy (TIRFM) (34) in combination with single-molecule detection (35) to investigate the mechanisms and dynamics of IgG exocytosis in live endothelial cells. For TIRFM, only a thin layer on the underside of the cell (adjacent to the coverslip) is illuminated, so that membrane proximal events such as exocytosis can be observed with minimal interference due to intracellular fluorescence (34, 36, 37). In contrast to the use of more conventional imaging approaches for which averaged signals from a large number of molecules are visualized, the use of single-molecule detection has allowed us to analyze the properties of individual IgG and FcRn molecules as they undergo exocytosis. Importantly, it has also resulted in the visualization of previously unidentified exocytic processes that would not be detected by using more standard methods that have to date been used in other systems.

This paper was submitted directly (Track II) to the PNAS office.

Abbreviations: FcRn, neonatal Fc receptor; TIRFM, total internal reflection microscopy.

‡To whom correspondence should be addressed. E-mail: sally.ward@utsouthwestern.edu.

www.pnas.org/cgi/doi/10.1073/pnas.0402970101

Our analyses show that there are multiple types of exocytic processes that can be distinguished, based on the extent and time frame of membrane fusion at the exocytic site. At one extreme, we observe a novel exocytic mode that is distinct from kiss-and-run events. In this mode, which we have designated "prolonged release," membrane-proximal compartments release IgG molecules over extended periods in multiple steps that appear to occur in a periodic fashion. At the other end of the spectrum of events, an exocytic mode can be observed that represents the classical model of exocytosis (22), involving complete collapse of the exocytic vesicle or tubule into the membrane with rapid release of FcRn and IgG. Our data also indicate that at least during the early stages of exocytosis, IgG molecules may be associated with membrane bound FcRn. Unexpectedly, after diffusion away from the epicenter of exocytic release, both FcRn and IgG can return to this site. Our studies provide insight into the dynamic processes that are involved in exocytosis of intracellularly transported IgG, in addition to being of more general significance to understanding exocytic mechanisms.

Materials and Methods

Plasmids, Antibodies, and Reagents. Expression constructs for human FcRn α-chain with a C-terminal fusion of enhanced GFP and human β2-microglobulin have been described (20). Human IgG1 [HuLys10 (38)] and a mutated derivative in which His-435 has been converted to alanine [H435A (11)] were purified as described (11). IgG was labeled with Alexa 546 carboxylic acid (succimidyl ester) (Molecular Probes) by using described methods (20).

Cells and Transfections. The human endothelial cell line HMEC-1.CDC [(39), a dermal-derived microvasculature cell line] was generously provided by F. Candal at the Centers for Disease Control (Atlanta). HMEC-1 cells were maintained and transiently transfected with expression constructs (1–2 μg of each) by using Nucleofector technology (Amaxa Biosystems, Cologne, Germany) as described (20). Immediately after transfection, cells were plated on coverslips in Phenol red-free Ham's F-12K medium. Cells were pulsed with labeled IgGs as in ref. 20.

Microscopy. Series images were acquired by using a Zeiss Axiovert 100TV inverted fluorescence microscope fitted with an Olympus (Melville, NY) 100× (1.65 numerical aperture) apochromatic objective and a Zeiss 1.6× Optovar. By using a custom-built right-side-facing filter cube, two laser lines were used for TIRFM excitation: a 488-nm laser (Laser Physics, West Jordan, UT) and a 543-nm laser (Research Electro-Optics, Boulder, CO). A Zeiss dual-video adaptor was used to permit the acquisition with two cameras. Images were acquired with two intensified cameras [I-PentaMax, Roper Scientific (Trenton, NJ) and Hamamatsu Sitcam C2400–08 (Bridgewater, NJ)].

The dual-color live-cell experiments were acquired with 100-ms exposure time settings for the I-PentaMax and 33-ms exposure times for the Sitcam camera at a frame rate of 10 frames per second. Because the I-PentaMax camera has lower noise characteristics, this camera was typically used to acquire the data from the channel that required the highest sensitivity. The single-color live-cell experiments were imaged with the I-PentaMax camera by using 50-ms exposure times. The single-color acquisition allowed for the use of wider emission filters, resulting in improved signal collection.

All data were processed and displayed by using a custom-written MIATOOL software package, which can be accessed at www2.utsouthwestern.edu/wardlab, in the high-level programming language MATLAB (Mathworks, Natick, MA). For image registration of dual-color image series, a test sample was produced with 100-nm four-color beads (TetraSpeck, Molecular Probes) that was used as a template to achieve image registration between the two cameras. The images resulting from the Sitcam camera were registered with those acquired on the I-PentaMax camera in MATLAB by using polynomial and linear registration algorithms. If necessary, for overlay images, the intensities of the individual components were adjusted to be of similar levels by using linear transformation of the pixel values.

Exocytic events were identified by visual inspection of the images. Fluorescence intensities were measured by summing the pixel values of 20 × 20 pixel arrays that contain the events of interest. Diffusion coefficients were calculated by using standard methods (40). For verification of single-molecule signal levels in the live-cell samples, GFP molecules and Alexa 546-labeled IgG molecules were immobilized on cover glasses and imaged under identical acquisition parameters to those used for the live-cell experiments. Single molecules showed the characteristic quantum drop in the signal level at photobleaching.

Results

Prolonged-Release and Complete-Fusion Modes of Exocytosis Are Responsible for IgG Exocytosis. The dermally-derived endothelial cell line (HMEC-1) was used throughout these studies. After transfection with FcRn-GFP, these cells can be used to analyze the intracellular sorting of IgGs with different affinities for FcRn (20). More specifically, IgGs that bind to FcRn are sorted away from the lysosomal pathway, whereas IgGs that do not bind are destined for lysosomal degradation (20, 21). The goal of the current study was to analyze exocytosis of IgG at the surface of FcRn-GFP-transfected HMEC-1 cells.

FcRn-GFP-transfected cells were pulsed with Alexa 546-labeled IgG (human IgG1), IgG was washed out, and the cells were imaged by using dual-color TIRFM. The use of dual-color TIRFM allowed us to simultaneously visualize FcRn-GFP and Alexa 546-labeled IgG in proximity to the plasma membrane. Multiple types of exocytic events can be seen and examples are shown in Fig. 1 *A* and *B*. In addition, exocytosed IgG was analyzed at the single-molecule level. For some exocytic events, complete fusion of the FcRn-GFP-positive vesicle or tubule with the membrane occurs (Fig. 1*A*). In such events, a brightening of the FcRn-GFP fluorescence occurs as the vesicle approaches the plasma membrane. This brightening is followed by a "puff" of green fluorescence that rapidly diffuses out into the membrane. Simultaneous with the green fluorescence diffusing into the membrane, the release of single IgG molecules occurs (Fig. 1*A*, and Movie 1, which is published as supporting information on the PNAS web site). At the other end of the spectrum of types of exocytic events to complete fusion, FcRn-GFP-positive compartments also exocytose IgG, whereas the FcRn-containing vesicle does not collapse into the membrane (Fig. 1*B*, and Movie 2, which is published as supporting information on the PNAS web site). Single IgG molecules released through this route are exocytosed in multiple pulses over extended periods. To distinguish this release mode from more rapid exocytic events involving complete fusion (Fig. 1*A*) or kiss and run (23–30), we refer to this mode as prolonged release.

Taken together, the dual-color TIRFM data indicate that different exocytic modes exist that result in the release of intracellular IgG. All events were observed multiple times. However, complete-fusion events were observed more frequently than prolonged-release events. Significantly, both complete-fusion and prolonged-release events can be seen in close proximity to each other in an individual cell (data not shown), indicating that the release mode does not depend on the physiological state of the cell. In addition to pulsing transfected HMEC-1 cells with human IgG1, cells were pulsed with Alexa-labeled H435A mutant, which has been shown in earlier studies to bind with very low affinity to FcRn (11). Dual-color TIRFM analyses indicated that at least 50 times lower numbers of H435A molecules were exocytosed relative to wild-type human IgG1

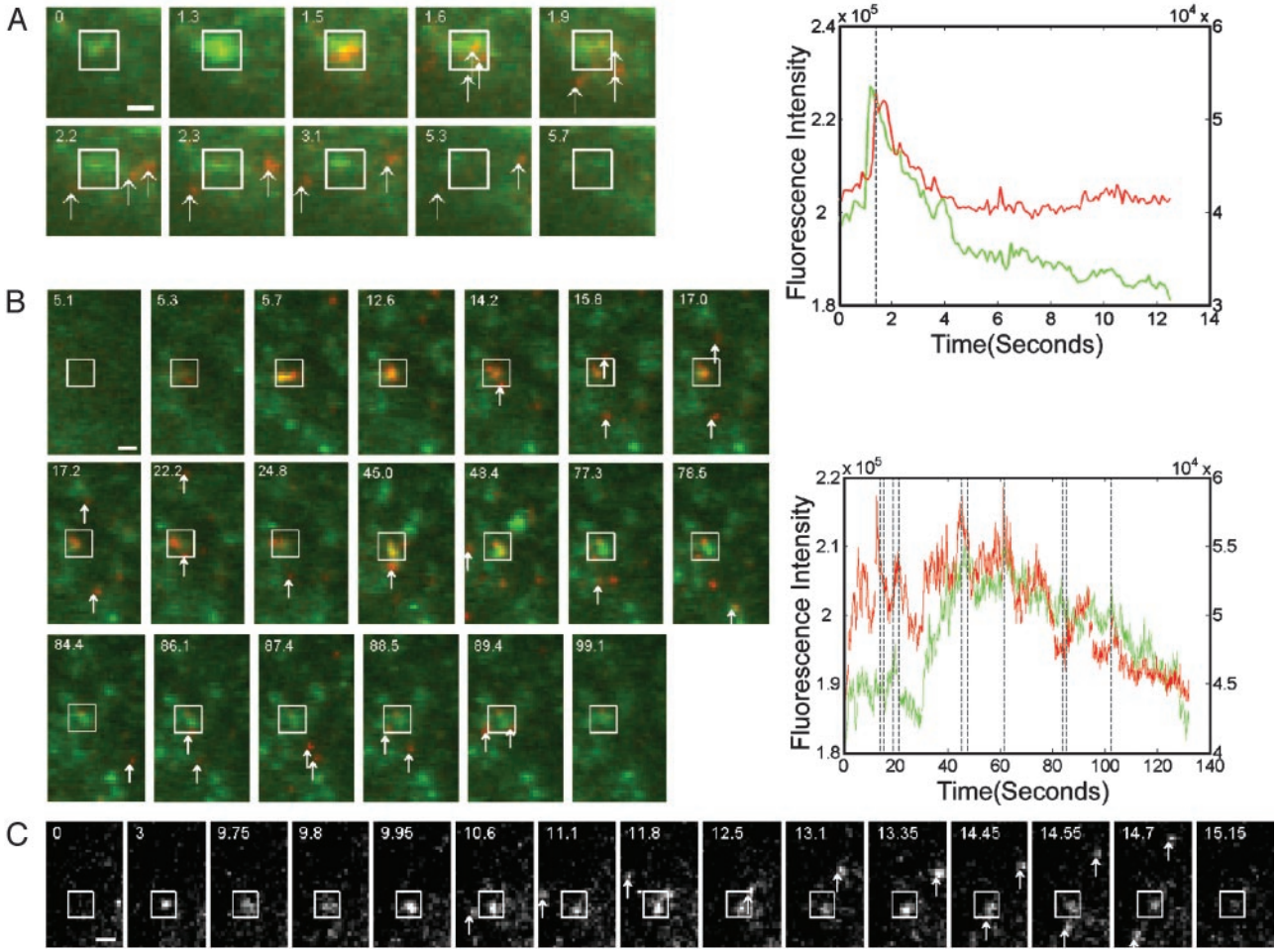

Fig. 1. Exocytic events in FcRn-GFP-transfected HMEC-1 cells. (*A* and *B*) Cells were pulsed with 1 mg/ml Alexa 546-labeled IgG for 60 min, were washed, and were then imaged by using dual-color TIRFM. (*C*) FcRn-GFP-transfected cells were imaged by using single-color TIRFM. Individual frames showing areas of interest of the cell surface are shown, with the time (in seconds) at which each frame was taken indicated (first frame is arbitrarily set to time 0, except for *B*, where time 0 corresponds to start of intensity plot). The exocytic sites are indicated by boxes within these images. The complete cell images from which the images in *A* and *B* are derived are shown in Fig. 4, which is published as supporting information on the PNAS web site). (*A*) Complete fusion of exocytic compartment with plasma membrane, resulting in a single release of three IgG molecules. (*B*) Prolonged release, with IgG-release events at 14.2, 15.8, 22.2, 48.4, 77.3, and 86.1 s. For *A* and *B*, arrows indicate individual IgG molecules (Alexa 546-labeled, red) and FcRn-GFP is green. Plots in *A* and *B* show GFP (FcRn, green) and Alexa 546 (IgG, red) fluorescence intensities at the exocytic site as a function of time for each type of release event. Vertical dashed lines indicate times at which IgG molecules emerged from the exocytic site (for *B*, not all IgG-release events are shown in the individual frames, but these results can be seen in Movie 2). (*C*) Pulses of FcRn-GFP release from an FcRn-GFP-positive compartment (release events at 10.6, 12.5 and 14.45 s). Arrows indicate single FcRn-GFP molecules. (Bars, 1 μm.) Movies 1, 2, and 3 correspond to Fig. 1 *A*, *B*, and *C*, respectively.

molecules. This marked difference is consistent with the relative binding affinities of the labeled IgGs, which were compared by using surface plasmon resonance and immobilized human FcRn (data not shown).

Periodicity of Prolonged-Release Events. For the prolonged-release events, we also investigated whether there is a relationship between the pulses of IgG release and FcRn-GFP fluorescence at the exocytic site. These analyses indicate that IgG-release events frequently correlate with increases in FcRn-GFP fluorescence intensity in a cyclical fashion, with a periodicity of several seconds between each exocytic event (Fig. 1*B*). Thus, the fusion pore appears to be able to undergo cycles of opening and closure. Moreover, the increases in FcRn-GFP fluorescence might be due to the exocytic compartment moving toward the plasma membrane. These processes result in quantized release of IgG through multiple release steps that occur over prolonged time periods. This result contrasts markedly with the single burst of IgG release that occurs during complete-fusion events (Fig. 1*A*). Significantly, we could also observe FcRn-GFP molecules being released in pulses from an FcRn-GFP-positive compartment during the imaging of FcRn-GFP-transfected cells at the single-molecule level (Fig. 1*C*, and Movie 3, which is published as supporting information on the PNAS web site). This finding suggests that even during the prolonged-release mode where the exocytic compartment does not completely fuse with the plasma membrane, FcRn-GFP molecules can diffuse out into the membrane.

Partial-Fusion Events Can Be Observed. In Fig. 1*A*, we show that complete-fusion events result in reduction of FcRn-GFP and IgG fluorescence levels to background levels at the exocytic site. However, this complete loss of fluorescence signal is not always seen. By using dual-color TIRFM, we observe that IgG and FcRn-GFP can be released at an exocytic site by means of a process that appears to involve fusion of the exocytic vesicle with the plasma membrane, but that both IgG and FcRn fluorescence persist in the vicinity of the exocytic site (Fig. 2*A*, and Movie 4,

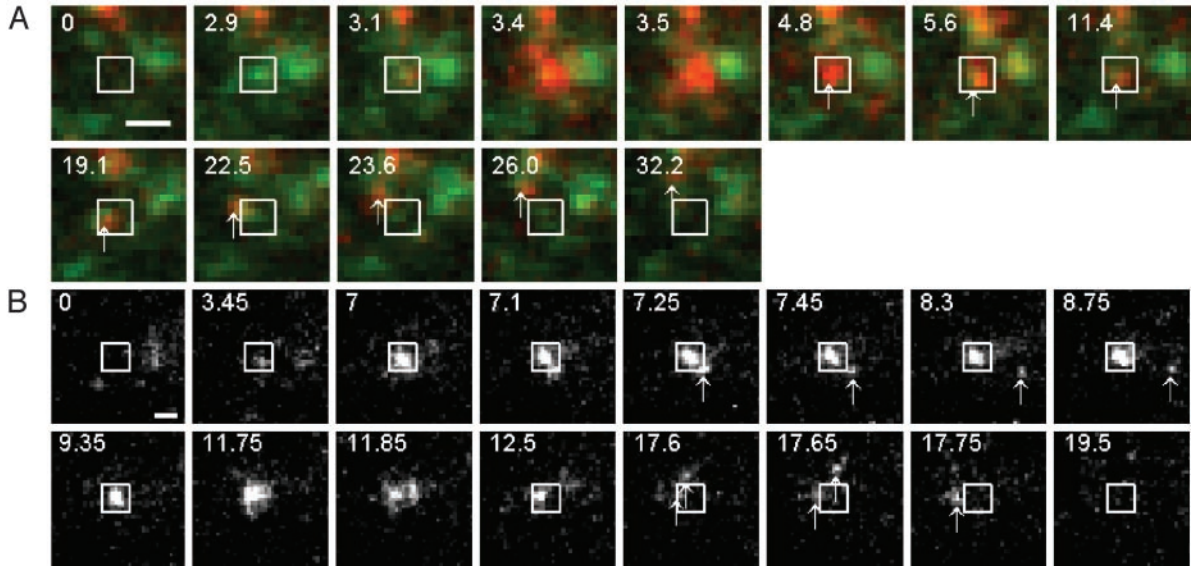

Fig. 2. Exocytic events involving partial release of FcRn and IgG can occur. Individual frames from areas of interest are shown, with the time in seconds at which each frame was taken (first frame is arbitrarily set to time 0). The boxes show the exocytic sites. (*A*) Dual-color TIRFM analyses of FcRn-GFP-transfected HMEC-1 cells pulsed with 1 mg/ml Alexa 546-labeled IgG for 60 min, followed by washing. A partial release event starts at 3.4 s. Arrows indicate a red (Alexa 546) and green (GFP) fluorescent compartment that remains after exocytosis and subsequently moves out of the focal plane. (*B*) Single-color TIRFM of FcRn-GFP-transfected HMEC-1 cells showing release of a single FcRn-GFP molecule (7.25 s), followed by two sequential fusion events (starting at 11.75 and 17.6 s). Arrows indicate single FcRn-GFP molecules. (Bars, 1 μm.) Movies 4 and 5 correspond to Fig. 2 *A* and *B*, respectively.

which is published as supporting information on the PNAS web site). This finding suggests that only partial fusion occurs. In the example shown in Fig. 2*A*, the residual compartment is finally lost by movement back into the cell (Fig. 2*A*). In analyses of FcRn-GFP in single-color TIRFM experiments, we also observe that the initial fusion event can result in release of individual FcRn-GFP molecules, followed by incomplete flattening of the exocytic compartment to release additional FcRn-GFP into the plasma membrane. Subsequent to these exocytic events, residual fluorescence can still be seen at the exocytic site (Fig. 2*B*, and Movie 5, which is published as supporting information on the PNAS web site). However, and in contrast to Fig. 2*A*, a subsequent fusion event results in rapid release of all remaining fluorescent material. Although the data in Fig. 2 *A* and *B* suggest partial-fusion events, some of which may occur repeatedly (Fig. 2*B*), an alternative possibility that cannot be excluded is that the residual fluorescence is due to the presence of a distinct (exocytic) compartment in close proximity to the fusion site. If this possibility is the case, it suggests that repeated exocytic events involving discrete vesicles/tubules can occur at the same site in the membrane.

Retrograde Movement of IgG and FcRn Molecules Back into the Epicenter of the Exocytic Site. The pathways taken by exocytosed IgG molecules were also analyzed (Fig. 3). Interestingly, in some cases, we observed tracking of IgG molecules back into the center of the exocytic site after initial diffusion away from the site (Fig. 3*B Center* and *Right*). Similarly, FcRn-GFP molecules can also sometimes move back toward the exocytic site (Fig. 3*C Right*). Single IgG molecules could be tracked for an average of 5.7 s, whereas single FcRn molecules could be tracked for an average of slightly <1 s, reflecting the fact that Alexa 546 has a lower rate of photobleaching than GFP. Taken together with our observation that the diffusion rates of IgG and FcRn-GFP molecules during exocytic events do not differ significantly (0.31 ± 0.2 $\mu m^2/s$ for IgG molecules, and 0.42 ± 0.22 $\mu m^2/s$ for exocytosed FcRn-GFP), this finding indicates that IgG molecules may be bound to FcRn-GFP for at least several seconds after membrane fusion. In fact, the measured diffusion rates for the IgG molecules are significantly lower than what would be expected if the molecules were diffusing freely (41).

It is known that FcRn binds to IgG in a pH-dependent way, with relatively strong binding at pH 6.0 that becomes progressively weaker as near-neutral pH is approached (42–44). Consistent with the possibility indicated by our single-molecule studies that IgG and FcRn molecules can remain associated during the early postexocytic phase, surface plasmon resonance analyses demonstrate that human IgG1 dissociates from immobilized FcRn at pH 7.2 in a period spanning several seconds (data not shown). Taken together, our observations indicate that plasma membrane bound IgG–FcRn complexes can be present during the initial stages (first few seconds) of exocytosis.

Discussion

We have analyzed the trafficking of human FcRn and its IgG ligand in transfected endothelial cells, with a particular focus on the exocytic pathways that lead to IgG release. Imaging of FcRn-GFP and IgG at the single-molecule level has allowed us to visualize events that would not be visible with more conventional, bulk fluorescence analyses. Our study therefore gives insight into the processes that lead to IgG exocytosis. In turn, this study has relevance to understanding how IgG is transported to diverse body sites. More generally, our analyses provide insight into mechanisms of exocytic processes that are involved in ligand recycling.

The current study indicates that FcRn-mediated exocytosis of IgG occurs through at least two modes. One mode involves complete fusion and dispersal of FcRn-GFP into the plasma membrane with simultaneous release of IgG. As a consequence, IgG release is relatively rapid. Significantly, we describe a second type of exocytic process, termed prolonged release, in which pulses of IgG release can occur over relatively long periods of time. These pulses of release frequently appear to occur simultaneously with the exocytic compartment approaching, but not fully dispersing into, the plasma membrane. Analyses of FcRn-GFP at the single-molecule level indicate that this type of

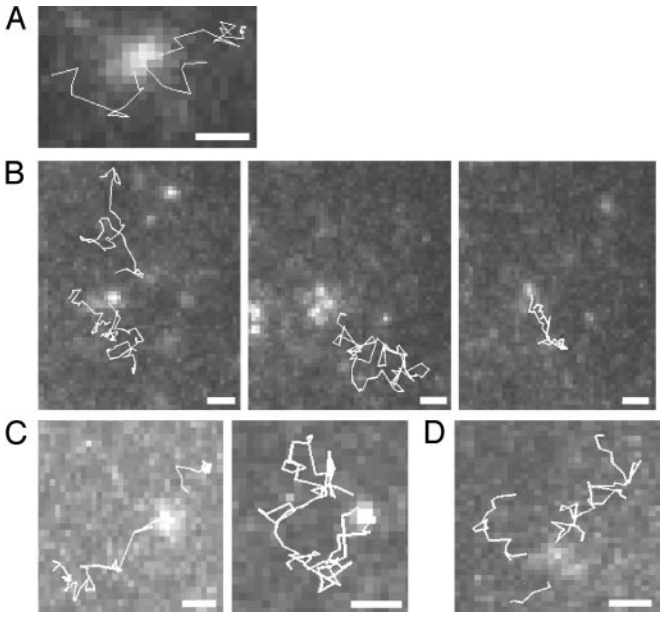

Fig. 3. Tracks of individual IgG and FcRn-GFP molecules after exocytic events. (*A* and *B*) FcRn-GFP-transfected HMEC-1 cells were pulsed in 1 mg/ml Alexa 546-labeled IgG, were washed, and were then imaged by using dual-color TIRFM. (*C* and *D*) FcRn-GFP-transfected cells were imaged by using single-color TIRFM. (*A*) Three tracks of single IgG molecules during a complete-fusion event superimposed on the image of the event at the moment of fusion. (*B Left*) Four tracks of single IgG molecules during a prolonged-release event superimposed on an image of the exocytic site. (*Center* and *Right*) The movement of IgG molecules back toward the exocytic site is shown, and the data are taken from a later stage of the prolonged-release event shown at *Left*. (*C*) Three tracks of FcRn-GFP molecules during a complete-fusion event superimposed on the image of the event at the moment of fusion. (*Right*) Movement of an FcRn-GFP molecule back toward the exocytic site. (*D*) Three tracks of single FcRn-GFP molecules during a prolonged-release event superimposed on an image of the exocytic site. (Bars, 1 μm.)

exocytic event can also involve the release of a proportion of the FcRn-GFP content of the exocytic compartment. For prolonged-release events, FcRn-GFP-positive compartments can persist in the vicinity of the fusion site after all detectable IgG has been released, distinguishing these processes from kiss-and-run models in which the exocytic vesicle recycles rapidly after fusion (23–30, 45). In addition, in two systems of regulated exocytosis where cargo release is followed by persistence of the exocytic compartment in the vicinity of the membrane, only a single pulse of release was reported (26, 28). Thus, the prolonged receptor-mediated release of pulses of ligand has not, to our knowledge, been described. In this context, identification of prolonged-release events is made possible in the current study by carrying out dual-color TIRFM, which allows both ligand and receptor to be simultaneously observed. In turn, this approach allows the prolonged-release events to be distinguished from other types of cellular events, whereas such a distinction would not be achievable by using single-color imaging modalities.

We have also observed exocytic processes that appear to result in only partial collapse of the exocytic vesicle or tubule into the plasma membrane. These events are characterized by rapid release of FcRn and IgG, followed by persistence of IgG and/or FcRn fluorescence in the vicinity of the exocytic site. In some cases, this fluorescence can be lost by a second exocytic event, whereas in others the fluorescently labeled compartment moves back into the cell. These phenomena are consistent with a model for IgG exocytosis in which the exocytic compartment can undergo various degrees of fusion with the plasma membrane and where partial, stepwise fusion events can occur repeatedly over a prolonged period. Significantly, our data also indicate that even for slower-release modes that do not involve complete collapse into the plasma membrane, a proportion of FcRn-GFP molecules can disperse from the exocytic site into the plasma membrane. Based on our observations, we suggest that rather than categorization of exocytic events into two discrete modes (complete fusion and prolonged release), the exocytic events may be interrelated and only distinguished by the extent and timing of membrane merging at the fusion site. Our data therefore contrast with the descriptions of regulated exocytosis in other systems (25–29, 31–33), where in general, types of exocytosis have been discretely categorized into either kiss-and-run or complete-fusion events. This apparent discrepancy is most likely due to the increased sensitivity of detection that is used here, together with the simultaneous analysis of ligand and receptor release. However, it is also possible that there is variation due to the different systems being analyzed.

The question arises as to what factors determine the type of exocytic event that occurs? Much data support the involvement of soluble *N*-ethylmaleimide-sensitive factor attachment protein receptors (SNAREs) in membrane fusion during exocytosis (46). There is also evidence indicating that dynamin may regulate fission of exocytic vesicles (29, 47), in addition to its established role in clathrin mediated endocytosis (48). In the simplest model, it is therefore possible that the type of exocytic event that occurs is determined by the relative activities of SNAREs, dynamin, and other relevant effectors, in the vicinity of the exocytic site. It is interesting that we observe cycles of release and retrieval with a periodicity of several seconds. This finding leads to the possibility that there are oscillating levels of relevant effectors for fusion or fission in proximity to the membrane fusion site.

Endothelial cells normally grow in polarized fashion with apical and basolateral surfaces, whereas they have been imaged as subconfluent monolayers here. When subconfluent, it is possible that, as for some epithelial cells (49), the HMEC-1 cells have some polarized character, and consequently, we are observing exocytic events primarily at the basolateral surface. It is conceivable that the frequencies and even types of exocytic events in HMEC-1 cells might differ at the two distinct surfaces in polarized endothelial cells. In this context, human FcRn is expressed predominantly on the basolateral relative to the apical surface of polarized Madin–Darby canine kidney cells (50).

Unexpectedly, we show that after an exocytic event, single IgG and FcRn-GFP molecules can sometimes return to the epicenter of the release site. The diffusion rates of IgG and FcRn-GFP molecules also do not differ significantly. Taken together with the observation that even prolonged-release modes are associated with some FcRn-GFP diffusion into the plasma membrane, our analyses suggest that during the first few seconds of exocytosis, IgG molecules can be bound to FcRn. This result is counter to existing models for FcRn function, where membrane fusion and IgG release are simultaneous. However, although the affinity of human IgG1 for FcRn at near-neutral pH is substantially lower than at pH 6.0 (51), surface plasmon resonance experiments with immobilized FcRn indicate that dissociation at this pH still takes several seconds (J.Z. and E.S.W., unpublished observations). Moreover, it is possible that the pH in the vicinity of the membrane is lower than 7.4 (the pH of the medium) due to the activity of Na^+/H^+ exchangers that are expressed in endothelial cells (52), which would in turn result in slower release. The retrograde movement of FcRn and IgG has important implications: first, this movement may serve as a retrieval mechanism for FcRn, for which the plasma membrane levels are generally maintained at low levels (1–5, 17). Second, the movement of FcRn-associated IgG back into the cell might be predicted to be more probable under conditions of high extracellular IgG concentrations. This event might then enhance the IgG load that is taken up. Alternatively, retrograde IgG move-

ment might be an undesirable consequence of rapid FcRn retrieval before complete dissociation of IgG. Nevertheless, our data suggest that even in an extracellular milieu of near-neutral pH, it is possible for IgG to enter endothelial cells by receptor-mediated, in addition to the previously assumed fluid phase (7), endocytic routes.

The existence of a variety of exocytic modes has implications for IgG homeostasis. More specifically, as endothelial cells are apposed to serum on the apical surface and to the interstitial space on the basolateral surface, both of which contain IgGs, prolonged-release modes would be predicted to sample the IgG concentration in the vicinity of the exocytic site, and also reduce the need for retrieval of FcRn-GFP from the plasma membrane. Depending on the vesicular/tubular IgG concentration immediately before exocytosis, net uptake or release of IgG could occur. As a result, fluid phase uptake of IgG and exocytic release could be coupled, and this uptake might be an efficient way of maintaining IgG homeostasis. In addition, prolonged release would avoid rapid fluxes in local IgG concentrations. It is therefore tempting to speculate that complete fusion, which would also be expected to be energetically less favorable, might represent an aberration of the regulation of exocytosis. Independent of the reason for the different types of ligand release, our data clearly show that exocytic modes other than complete fusion are not solely restricted to regulated exocytosis where rapid retrieval after release has been argued to be advantageous (30). We would predict that the types of exocytic events described here are generally relevant to many cell types that may not necessarily be specialized toward regulated exocytic functions, such as neurotransmitter release. Future studies will be directed toward delineating the factors that regulate the exocytic pathways taken by transported IgG molecules.

We thank Palmer Long for expert assistance, Francisco Candal for providing HMEC-1, Dr. Jefferson Foote for providing human IgG1 expressing cells and vectors, and Drs. Michael Roth and Ege Kavalali for helpful discussions. This work was supported by National Institutes of Health Grants R01 AI39167, R01 AI50747, and R21 AI53748.

1. Praetor, A., Ellinger, I. & Hunziker, W. (1999) *J. Cell Sci.* **112,** 2291–2299.
2. McCarthy, K. M., Yoong, Y. & Simister, N. E. (2000) *J. Cell Sci.* **113,** 1277–1285.
3. Dickinson, B. L., Badizadegan, K., Wu, Z., Ahouse, J. C., Zhu, X., Simister, N. E., Blumberg, R. S. & Lencer, W. I. (1999) *J. Clin. Invest.* **104,** 903–911.
4. Claypool, S. M., Dickinson, B. L., Yoshida, M., Lencer, W. I. & Blumberg, R. S. (2002) *J. Biol. Chem.* **277,** 28038–28050.
5. Antohe, F., Radulescu, L., Gafencu, A., Ghetie, V. & Simionescu, M. (2001) *Hum. Immunol.* **62,** 93–105.
6. Kobayashi, N., Suzuki, Y., Tsuge, T., Okumura, K., Ra, C. & Tomino, Y. (2002) *Am. J. Renal Physiol.* **282,** F358–F365.
7. Ghetie, V. & Ward, E. S. (2000) *Annu. Rev. Immunol.* **18,** 739–766.
8. Ravetch, J. V. & Bolland, S. (2001) *Annu. Rev. Immunol.* **19,** 275–290.
9. Medesan, C., Matesoi, D., Radu, C., Ghetie, V. & Ward, E. S. (1997) *J. Immunol.* **158,** 2211–2217.
10. Ellinger, I., Schwab, M., Stefanescu, A., Hunziker, W. & Fuchs, R. (1999) *Eur. J. Immunol.* **29,** 733–744.
11. Firan, M., Bawdon, R., Radu, C., Ober, R. J., Eaken, D., Antohe, F., Ghetie, V. & Ward, E. S. (2001) *Int. Immunol.* **13,** 993–1002.
12. Spiekermann, G. M., Finn, P. W., Ward, E. S., Dumont, J., Dickinson, B. L., Blumberg, R. S. & Lencer, W. I. (2002) *J. Exp. Med.* **196,** 303–310.
13. Rodewald, R. & Kraehenbuhl, J. P. (1984) *J. Cell Biol.* **99,** 159s–164s.
14. Simister, N. E. & Rees, A. R. (1985) *Eur. J. Immunol.* **15,** 733–738.
15. Roberts, D. M., Guenthert, M. & Rodewald, R. (1990) *J. Cell Biol.* **111,** 1867–1876.
16. Israel, E. J., Patel, V. K., Taylor, S. F., Marshak-Rothstein, A. & Simister, N. E. (1995) *J. Immunol.* **154,** 6246–6251.
17. Ghetie, V., Hubbard, J. G., Kim, J. K., Tsen, M. F., Lee, Y. & Ward, E. S. (1996) *Eur. J. Immunol.* **26,** 690–696.
18. Junghans, R. P. & Anderson, C. L. (1996) *Proc. Natl. Acad. Sci. USA* **93,** 5512–5516.
19. Israel, E. J., Wilsker, D. F., Hayes, K. C., Schoenfeld, D. & Simister, N. E. (1996) *Immunology* **89,** 573–578.
20. Ober, R. J., Martinez, C., Vaccaro, C., Zhou, J. & Ward, E. S. (2004) *J. Immunol.* **172,** 2021–2029.
21. Ward, E. S., Zhou, J., Ghetie, V. & Ober, R. J. (2003) *Int. Immunol.* **15,** 187–195.
22. Heuser, J. E. & Reese, T. S. (1973) *J. Cell Biol.* **57,** 315–344.
23. Fesce, R. & Meldolesi, J. (1999) *Nat. Cell Biol.* **1,** E3–E4.
24. Ceccarelli, B., Hurlbut, W. P. & Mauro, A. (1973) *J. Cell Biol.* **57,** 499–524.
25. Albillos, A., Dernick, G., Horstmann, H., Almers, W., Alvarez de Toledo, G. & Lindau, M. (1997) *Nature* **389,** 509–512.
26. Tsuboi, T., Zhao, C., Terakawa, S. & Rutter, G. A. (2000) *Curr. Biol.* **10,** 1307–1310.
27. Tsuboi, T. & Rutter, G. A. (2003) *Curr. Biol.* **13,** 563–567.
28. Taraska, J. W., Perrais, D., Ohara-Imaizumi, M., Nagamatsu, S. & Almers, W. (2003) *Proc. Natl. Acad. Sci. USA* **100,** 2070–2075.
29. Holroyd, P., Lang, T., Wenzel, D., De Camilli, P. & Jahn, R. (2002) *Proc. Natl. Acad. Sci. USA* **99,** 16806–16811.
30. Schneider, S. W. (2001) *J. Membr. Biol.* **181,** 67–76.
31. Ales, E., Tabares, L., Poyato, J. M., Valero, V., Lindau, M. & Alvarez de Toledo, G. (1999) *Nat. Cell Biol.* **1,** 40–44.
32. Zenisek, D., Steyer, J. A. & Almers, W. (2000) *Nature* **406,** 849–854.
33. Lampson, M. A., Schmoranzer, J., Zeigerer, A., Simon, S. M. & McGraw, T. E. (2001) *Mol. Biol. Cell* **12,** 3489–3501.
34. Steyer, J. A. & Almers, W. (2001) *Nat. Rev. Mol. Cell Biol.* **2,** 268–275.
35. Sako, Y. & Yanagida, T. (2003) *Nat. Rev. Mol. Cell Biol.* Suppl., SS1-SS5.
36. Toomre, D., Steyer, J. A., Keller, P., Almers, W. & Simons, K. (2000) *J. Cell Biol.* **149,** 33–40.
37. Schmoranzer, J., Goulian, M., Axelrod, D. & Simon, S. M. (2000) *J. Cell Biol.* **149,** 23–32.
38. Foote, J. & Winter, G. (1992) *J. Mol. Biol.* **224,** 487–499.
39. Pruckler, J. M., Lawley, T. J. & Ades, E. W. (1993) *Pathobiology* **61,** 283–287.
40. Saxton, M. J. & Jacobson, K. (1997) *Annu. Rev. Biophys. Biomol. Struct.* **26,** 373–399.
41. Berg, H. C. (1993) *Random Walks in Biology* (Princeton Univ. Press, Princeton).
42. Rodewald, R. (1976) *J. Cell Biol.* **71,** 666–669.
43. Wallace, K. H. & Rees, A. R. (1980) *Biochem. J.* **188,** 9–16.
44. Raghavan, M., Bonagura, V. R., Morrison, S. L. & Bjorkman, P. J. (1995) *Biochemistry* **34,** 14649–14657.
45. Valtorta, F., Meldolesi, J. & Fesce, R. (2001) *Trends Cell Biol.* **11,** 324–328.
46. Sollner, T. H. (2003) *Mol. Membr. Biol.* **20,** 209–220.
47. Graham, M. E., O'Callaghan, D. W., McMahon, H. T. & Burgoyne, R. D. (2002) *Proc. Natl. Acad. Sci. USA* **99,** 7124–7129.
48. Conner, S. D. & Schmid, S. L. (2003) *Nature* **422,** 37–44.
49. Brown, P. S., Wang, E., Aroeti, B., Chapin, S. J., Mostov, K. E. & Dunn, K. W. (2000) *Traffic* **1,** 124–140.
50. Claypool, S. M., Dickinson, B. L., Wagner, J. S., Johansen, F.-E., Venu, N., Borawski, J. A., Lencer, W. I. & Blumberg, R. S. (2004) *Mol. Biol. Cell* **15,** 1746–1759.
51. Zhou, J., Johnson, J. E., Ghetie, V., Ober, R. J. & Ward, E. S. (2003) *J. Mol. Biol.* **332,** 901–913.
52. Hattori, R., Otani, H., Moriguchi, Y., Matsubara, H., Yamamura, T., Nakao, Y., Omiya, H., Osako, M. & Imamura, H. (2001) *Am. J. Physiol.* **280,** H2796–H2803.